



Original Article

BTF3L4 Overexpression Mediates APAP-induced Liver Injury in Mouse and Cellular Models



Junchao Lin^{1#}, Aqiang Fan^{2#}, Zhujiu Yifu², Qibing Xie², Liu Hong^{2*}  and Wei Zhou^{2*}

¹State Key Laboratory of Cancer Biology, National Clinical Research Center for Digestive Diseases and Xijing Hospital of Digestive Diseases, Air Force Military Medical University, Xi'an, Shaanxi, China; ²Department of Digestive Surgery, Xijing Hospital, Air Force Military Medical University, Xi'an, Shaanxi, China

Received: 13 August 2023 | Revised: 1 November 2023 | Accepted: 17 November 2023 | Published online: 8 February 2024

Abstract

Background and Aims: Acetaminophen (APAP)-induced liver injury (AILI) has an increasing incidence worldwide. However, the mechanisms contributing to such liver injury are largely unknown and no targeted therapy is currently available. The study aimed to investigate the effect of BTF3L4 overexpression on apoptosis and inflammation regulation *in vitro* and *in vivo*. **Methods:** We performed a proteomic analysis of the AILI model and found basic transcription factor 3 like 4 (BTF3L4) was the only outlier transcription factor overexpressed in the AILI model in mice. BTF3L4 overexpression increased the degree of liver injury in the AILI model. **Results:** BTF3L4 exerts its pathogenic effect by inducing an inflammatory response and damaging mitochondrial function. Increased BTF3L4 expression increases the degree of apoptosis, reactive oxygen species generation, and oxidative stress, which induces cell death and liver injury. The damage of mitochondrial function by BTF3L4 triggers a cascade of events, including reactive oxygen species accumulation and oxidative stress. According to the available AILI data, BTF3L4 expression is positively associated with inflammation and may be a potential biomarker of AILI. **Conclusions:** Our results suggest that BTF3L4 is a pathogenic factor in AILI and may be a potential diagnostic marker for AILI.

Citation of this article: Lin J, Fan A, Yifu Z, Xie Q, Hong L, Zhou W. BTF3L4 Overexpression Mediates APAP-induced

Liver Injury in Mouse and Cellular Models. *J Clin Transl Hepatol* 2024;12(3):245–256. doi: 10.14218/JCTH.2023.00342.

Introduction

Drug-induced liver injury (DILI) is a common cause of severe liver disease induced by medication exposure. Most DILI cases occur following an accidental overdose of acetaminophen (APAP), which is one of the most widely and safely used analgesic and antipyretic drugs for the treatment of agnogenic or incapacitating high fever.¹ APAP is safe at the therapeutic dosage level but an overdose can lead to hepatotoxicity and even acute liver failure, particularly in cases of high fever caused by COVID-19.^{2,3} However, owing to its insidious onset, fast progress, and lack of specific biomarkers, the diagnosis and treatment of DILI are challenging for clinicians. The diagnosis of DILI depends on clinical, biochemical, and histologic information. N-acetylcysteine is the only clinical treatment option for DILI caused by an APAP overdose. As APAP has limitations that include a narrow therapeutic window and adverse effects, new, effective approaches and studies of the mechanisms of DILI are urgently required.^{4,5}

APAP-induced liver injury (AILI) is the predominant cause of DILI, and several studies have been conducted to explore its fundamental mechanisms.^{6–8} Excessive oxidative stress leads to mitochondrial dysfunction and c-Jun N-terminal kinase (JNK) overactivation, which is considered to be the major cause of APAP-induced cell death.^{6,9} APAP is absorbed in the gut, and most is metabolized in the liver by glucuronidation and sulfation while some is neutralized by glutathione (GSH).^{10,11} However, APAP overdose causes GSH exhaustion. Subsequently, increased generation of reactive oxygen species (ROS) facilitates the activation of a mitogen-activated protein kinase cascade that results in the phosphorylation of JNK. These changes inhibit electron transport and adenosine triphosphate synthesis that promotes ROS production.¹² Furthermore, excess ROS tolerates JNK activation and leads to the permeabilization and lysis of the mitochondrial membrane, which ultimately causes nuclear DNA fragmentation by originating intrinsic apoptotic pathways. The initiation of intrinsic apoptotic pathways aggravates hepatic cellular damage by altering mitochondrial homeostasis and promoting inflammatory responses. These processes collectively lead to centrilobular cell death and liver injury.^{6,13,14}

Transcription factors (TFs) are proteins that interact with

Keywords: BTF3L4; APAP-induced liver injury; Apoptosis; Mitochondrial morphology; Inflammation.

Abbreviations: AILI, acetaminophen-induced liver injury; ALT, alanine aminotransferase; AML-12, alpha mouse liver-12; APAP, acetaminophen; AUC, area under the receiver operating characteristic curve; BTF3, basic transcription factor 3; BTF3L4, basic transcription factor 3 like 4; DILI, drug-induced liver injury; GSH, glutathione; HE, hematoxylin and eosin; HMGB1, high mobility group box-1 protein; JNK, c-Jun N-terminal kinase; PBS, phosphate-buffered saline; PCNA, proliferating cell nuclear antigen; qPCR, real-time quantitative polymerase chain reaction; ROC, receiver operating characteristic; GEO, gene expression omnibus; ROS, reactive oxygen species; shRNA, short hairpin RNA; TBARS, thiobarbituric acid reactive substances; DAMP, damage associated molecular patterns; TEM, transmission electron microscopy; TF, transcription factor; TNF- α , tumor necrosis factor-alpha; IL-1 β , interleukin-1 β ; p-JNK, phospho-c-Jun N-terminal kinase; TUNEL, terminal deoxynucleotidyl transferase-mediated dUTP-biotin nick end labeling.

*Contributed equally to this work.

Correspondence to: Wei Zhou and Liu Hong, Department of Digestive Surgery, The Fourth Military Medical University, Xi'an, Shaanxi 710032, China. ORCID: <https://orcid.org/0000-0002-7611-1108> (LH). Tel: +86-29-84771532 (WZ and LH), Fax: +86-29-84771466 (WZ and LH), E-mail: 252376698@qq.com (WZ) and hongliu1@fmmu.edu.cn (LH)

other proteins and play a significant role in the basic transcription processes required for diverse biological functions.¹⁵ Among these TFs, basic transcription factor 3 (BTF3) is a highly focused TF owing to its role in transcription activation. An increasing number of studies have shown an association between the function of BTF3 and the development of digestive diseases.^{16,17} However, the association of the role of BTF3 with liver disorders is not completely understood. For instance, BTF3 is an oncogene in several digestive cancers. In pancreatic ductal adenocarcinoma, BTF3 is overexpressed and a key prognostic gene. Moreover, BTF3 overexpression is found in pancreatic ductal adenocarcinoma, which regulates several cancer-associated genes rather than acting as a direct modulator of apoptosis, leading to poor prognosis.¹⁷ BTF3 overexpression in colorectal cancer tissue is associated with poor patient survival as it influences the indicators of cancer including epithelial-mesenchymal transition, stem cell-like traits, proliferation, and migration.¹⁶ BTF3 is also involved in the development and progression of gastric cancer through the regulation of FOXM1 and JAK2/STAT3 signaling pathways.¹⁸ BTF3 downregulation induces mitochondrial dysfunction and intrinsic apoptosis in mouse liver cell lines, demonstrating its ability to maintain the homeostasis of liver cells.^{19,20} However, few studies have assessed the specific mechanism through which the BTF3 family of TFs regulates diseases, whether they function in AILI, and what that activity is.

We tested the hypothesis that BTF3L4 overexpression aggravates liver injury by upregulating the level of apoptosis and investigated whether the changes increase inflammation and necrosis in hepatic cells and lead to increased liver injury and illness. APAP was used to induce an AILI model of liver injury. Cells with BTF3L4 overexpression or BTF3L4 knock-down were constructed. We conducted molecular studies of the effects of BTF3L4 overexpression on the key pathogenic factors that were involved in regulating apoptosis and inflammation *in vitro*. We also assessed the pathogenic effects of BTF3L4-activated liver injury in an AILI model in mice, and explored the physiological significance of BTF3L4-induced apoptosis in a normal mouse cell line.

Methods

Mice

Wild-type C57BL/6 mice were purchased from the Experimental Animal Center of The Fourth Military Medical University (Certificate No. SCXK2012-0007). A total of 48 male mice between 8–12 weeks of age were used for these studies. The mice, weighing 20±3 g, were randomly divided into six groups of six mice each, as follows: a control group treated with phosphate-buffered saline (PBS), an APAP group treated for 3 h, an APAP group treated for 6 h, an APAP group treated for 12 h, an APAP group treated for 24 h, and an APAP group treated for 48 h. Mice were housed in a 12-hour light/dark cycle and given a standard diet, and drinking water was provided *ad libitum*.

Animal and cellular models of APAP-induced acute liver injury

For an animal model APAP-induced acute liver injury, mice were fasted overnight (~12 h) on new alpha-dry bedding before administration of 300 mg/kg APAP (30 µL/g body weight) or vehicle (warm PBS) by intraperitoneal injection as previously described.²¹ Feeding was resumed immediately after injection. Blood and liver samples were collected at 6, 24, or 48 h after APAP administration. Blood was collected under isoflurane anesthesia, from the heart using a syringe

containing heparin sodium (1% final concentration). Blood samples were centrifuged at 3,500 g for 15 m to obtain plasma and were stored at -80°C. Livers were rinsed in PBS and fixed in either 10% neutral-buffered formalin or snap-frozen in liquid nitrogen.

For a cellular model of APAP-induced acute liver injury, alpha mouse liver 12 (AML-12) cells were treated with APAP at a final concentration of 30 µM (APAP in PBS) or vehicle (PBS) as previously described.²² AML-12 cells were obtained from the Type Culture Collection of Chinese Academy of Sciences (Shanghai, China) and were cultured in Dulbecco's Modified Eagle Medium supplemented with 10% fetal bovine serum, 1% penicillin-streptomycin at 37 °C with 95% air and 5% CO₂.

Ethical approval of animal experiments

The study was approved by the Institutional Animal Care and Use Committee of the Fourth Military Medical University (No. IACU-20231007) following the ethical principles of animal welfare. A total of 48 C57BL/6 male mice were purchased from the Animal Center of the Fourth Military Medical University (Production License No. SCXK SHAN 2019-001). The experimental method involved intraperitoneal injection of APAP to induce liver injury *in vivo*. Euthanasia was performed by CO₂ inhalation followed by cervical dislocation. Liver tissue and serum were collected and weighed. After the experiments, all mice were properly disposed of. All procedures were conducted following the guidelines established by the Animal Care and Use Committee, with efforts made to minimize animal discomfort and reduce the number of animals sacrificed.

Measurement of cellular thiobarbituric acid reactive substances (TBARS)

Measuring TBARS is a well-established method for screening and monitoring lipid peroxidation. Cell lysates were prepared from 2 × 10⁷ AML-12 cells as previously described and not diluted before assaying. Colorimetric malondialdehyde assays were performed with TBARS assay kits (700870; Cayman, Ann Arbor, USA). AML-12 cells were collected and homogenized and culture medium was prepared as a sample blank before further use. Colorimetric standards, tricarboxylic acid assay reagent (10%), color reagent, and samples were added to each vial and vortexed. Each vial was boiled for 1 h and then incubated on ice for 10 m. After centrifuging the vials for 10 m at 1,600 g at 4°C, they were kept at room temperature for 30 m and then 200 µL of the mixture from each vial was transferred to a plate for reading on a Multiskan FC Microplate Photometer (1410101; Thermo Fisher Scientific, Waltham, USA) for reading at a wavelength of 535 nm. The final absorbance value of samples was calculated from a standard curve plotted using real-time standards supplied with the kit.

Immunohistochemistry and immunofluorescence

Immunohistochemistry and immunofluorescence were performed as previously described.²³ The primary antibodies were anti-BTF3L4 (ab128870; Abcam, Waltham, USA) and anti-albumin (ab106582; Waltham, USA). Briefly, formalin-fixed, paraffin-embedded liver tissue was sectioned, mounted on slides, and subjected to antigen retrieval in buffer according to the manufacturer's protocol; endogenous peroxidase activity was then blocked by incubating in 3% H₂O₂ for 15 m. The slides then were incubated with primary antibody overnight at 4°C followed by a 1-h incubation with fluorescence-labelled secondary antibodies (ab150075 and ab150113; Abcam). For hematoxylin and eosin (HE) and TUNEL staining, paraffin-embedded liver sections were stained with In Situ

Cell Death Detection TUNEL Kits (11684809910; Roche-Merck, Merck, Switzerland). Stained sections were visualized and analyzed with a confocal laser scanning microscope (FV-3000; Olympus, Tokyo, Japan).

CCK8 Assay

AML-12 cells were seeded into 96-well plates at a density of 8,000 cells per well. Subsequently, 10 μ L of CCK8 reagents (HY-K0301; MCE, New Jersey, USA) were added to each well under light-free conditions. The plates were then incubated at 37°C and 5% CO₂ for varying durations ranging from 1 to 7 hours. Finally, the optical densities of the wells were measured at a wavelength of 450 nm using a microplate reader. All experiments were performed in triplicate.

Cell transfection

To knock down BTF3L4 expression in AML-12 cells, lentiviral plasmid vectors encoding short hairpin RNAs (shRNAs) targeting BTF3L4 or negative control shRNA were generated and designated as shBTF3L4 and shNC, respectively.

Mouse BTF3L4 shRNA1: GCACGGTTATTTCATTCAACA; Mouse BTF3L4 shRNA2: GCTAACACCTTTGCAATTACT; Mouse BTF3L4 shRNA3: GCTTGGTGTGACAGCTTAAC. For overexpression of BTF3L4 in AML-12 cells, AML-12 cells were infected with adenoviruses expressing BTF3L4 (Ad-BTF3L4): ATGAATCAAGAAAAGTTAGCCAACTTCAAGCTCAGGTCCGGATAGGGGGCAAGGGTACAGCTCGCAGGAAGAAGAGGTGGTACATAGGACAGCTACTGCTGATGACAAAAGCTTCAGAGTTCAC-TAAAGAACTGGCTGTGAAACAATATAGCTGGTATTGAAGAGGTGAATATGATTAAGACGATGGCAGCGTTATTTCATTCAACAATCCCAAAGTCCAAGCTTCCCTCTCCGCTAACACCTTTGCAATTAATG-GTCATGCAGAAGCCAAACCAATCACAGAAATGTTCTCTGGGA-TATTAAGTCAGCTTGGTGCTGACAGCTTAACGAGCCTTAGAAA-GTTAGCTGAACAGTTCCACGGCAAGTATTGGATAGTAAAGCGCCCAAACCCAGAAGACATCGATGAAGAGGATGATGATGTTCCAGATCTTGTAGAAAATTTTGTATGAAGCATCGAAAAATGAAGCTAACGATTACAAGGATGACGACGATAAGGGAGATTA-CAAGGATGACGACGATAAGATCGATTACAAGGATGACGACGATAAGTAA, and Ad-NC as the control. The same protocol as described above was used for shRNAs against BTF3L4, Ad-BTF3L4, and a negative control but synthesized by Tsingke Biotechnology Co, Ltd. (Beijing, China). Transfection of cells was conducted following the manufacturer's instructions using Lipofectamine 3000 transfection reagent (Thermo Fisher Scientific). Efficiency of transfection was validated by real-time quantitative polymerase chain reaction (qPCR), protein extraction and western blotting.

Transmission electron microscopy (TEM)

Mitochondrial ultrastructure in a cellular model of APAP-induced acute liver injury was evaluated by TEM. The cell lines were harvested and fixed in 2.5% glutaraldehyde for 2 h at 4°C, post-fixed in 1% osmium tetroxide for 1 h at 4°C, dehydrated, and embedded in epoxy resin. Ultrathin 60–80 nm sections were cut with an ultramicrotome (RMC/MTX; Elxience, EM UC7 Ultramicrotome, Witzler in Hesse, Germany), mounted on copper grids, stained with 8% uranyl acetate and lead citrate, and observed with a JEM-1010 transmission electron microscope (JEOL, Tokyo, Japan). IMOD software (IMOD 4.10, University of Colorado Boulder, USA) was used to analyze images and delineate major cellular structures.

Flow cytometry

To determine ROS levels, cells were treated with 2',7'-dichlorodihydro fluorescein diacetate in 10 μ mol/L for 30 m at 37°C in the dark, washed twice with PBS, and digested with

trypsin. The level of apoptosis was determined by flow cytometric assay of intensity of intracellular ROS fluorescence. We used cell cycle and apoptosis detection kits (C1052; Beyotime Biotechnology, Shanghai, China) to evaluate the cell cycle by flow cytometry. After staining with 500 μ L propidium iodide solution at 37°C for 30 m, we performed flow cytometry (FACSVerse flow cytometer; BD Biosciences, Franklin Lake, New Jersey, USA) and the percentages of cells in various phases of the cell cycle were calculated with FlowJo software (Treestar, Ashland, OR, USA).

RNA isolation and real-time reverse transcription

RNA was isolated from liver tissue and cellular samples with TRIzol reagent (ThermoFisher, Waltham, USA) following the manufacturer's instructions. RNA concentration and quality were determined by Nanodrop 2000 (Thermo Fisher Scientific), and the complementary DNA was prepared as described above. qPCR was used to determine the mRNA levels of target genes using a Bio-Rad CFX384 touch real-time PCR detection system (Bio-Rad, Hercules, USA) with Maxima SYBR green qPCR reagents (ISO13485; Abm, Vancouver, Canada). Mouse 18S ribosomal RNA was used for normalization.

The primer sequences used for the mRNA assays were: Mouse 18S forward, 5'-AGGGGAGAGCGGGTAAGAGA-3'; Mouse 18S reverse, 5'-GGACAGGACTAGGCG-GAACA-3'; Mouse IL-1 β forward, 5'-GAAATGCCACCTTTGACAGTG-3'; Mouse IL-1 β reverse, 5'-TGGATGCTCTCATCAGGACAG-3'; Mouse tumor necrosis factor- α (TNF- α) forward, 5'-GATCGGTCCCAAAGGGATG-3'; Mouse TNF- α reverse, 5'-TTTGCTACGACGTGGGCTAC-3'; Mouse MCSFR forward, 5'-GAAGCACCTGACCACAAGA-3'; MCSFR reverse, 5'-AGAGTGGGCCGGATCTTTGA-3'; Mouse BTF3L4 forward, 5'-AGAAGGTGGTACATAGGACAGC-3'; and Mouse BTF3L4 reverse, 5'-CCGTGCCATCGTCTTTAATCAT-3'.

Protein extraction and western blotting

Nuclear and cytoplasmic protein extracts were prepared as previously described using nuclear and cytoplasmic protein extraction reagent kits (Beyotime Biotechnology) following the manufacturer's instructions.²³ The protein concentration was determined with bicinchoninic acid assay kits (Thermo Fisher Scientific). The proteins in samples of equal concentration were separated by 10% and 15% sodium dodecyl-sulfate polyacrylamide gel electrophoresis gels and transferred to a nitrocellulose membrane. After blocking, the membranes were incubated with primary antibodies at 4°C overnight. The next day, the membranes were incubated with the anti-rabbit secondary antibody for 1 h at room temperature. The protein bands were detected by chemiluminescence and the intensity was calculated by densitometry. Primary antibodies and working dilutions are detailed in Supplementary Table 1.

Gene Ontology enrichment analyses

The APAP-induced model mice and normal mouse liver tissue samples were submitted to Qinglian Biotech Co, Ltd, Beijing, China for LC-MS/MS analysis. Enrichment analysis was conducted using Gene Ontology (GO) analysis to investigate biological processes, molecular function, and cellular component. GEO dataset was downloaded from GEO database (<https://www.ncbi.nlm.nih.gov/>).

Statistical analysis

The data were reported as means \pm standard deviation. One-way analysis of variance was used for multiple-group comparisons and the least significant difference *t*-test was used for internal group comparisons. The statistical analysis was

performed with SPSS version 19 (IBM Corp., Armonk, NY, USA). The threshold of statistical significance was $p < 0.05$. GraphPad Prism version 6.02 (La Jolla, CA, USA) was used to generate histograms.

Results

BTF3L4 is overexpressed in APAP-induced DILI patients and in an animal model

We performed proteomic analysis of four APAP-induced model mice and normal mouse liver tissue samples. Gene Ontology cellular component enrichment of differentially expressed proteins identified the change of mitochondrial function as a core of physiological function altered in the AILI animal model (Fig. 1A). Among the upregulated proteins, BTF3L4 was the only one involved in regulating the activity of transcription, and it was overexpressed in all four paired APAP-induced mouse samples (Fig. 1B), with a 6.4-fold upregulation. First, the serum alanine aminotransferase (ALT) from different APAP-treated groups was determined. The mouse serum samples were collected at 6, 24, and 48 h after APAP treatment. The APAP-induced increase of serum of ALT, a marker of liver injury, was significantly increased in mice 6 h after APAP treatment compared with the control. However, serum ALT levels were lower at 48 h than after 24 h (Fig. 1C). Results of the protein and mRNA assays of BTF3L4 in APAP-induced mouse samples are shown in Figure 1D and E, respectively. BTF3L4 was significantly upregulated in mouse liver tissue compared with the control 3 h after APAP treatment. High mobility group box-1 protein (HMGB1) is a nuclear protein that is released during necrosis of most cell types and acts as a damage associated molecular patterns (DAMP) to activate innate immune cells. It is considered as a tentative biomarker for DILI. We also observed a significantly elevated mRNA expression of *Hmgb-1* in mouse liver tissue compared with controls 3 h after induction (Fig. 1F). Next, we analyzed the correlation between *Btf3l4* and *Hmgb1* mRNA expression in APAP-induced mouse model liver tissues. The mRNA level of *Btf3l4* was positively correlated with *Hmgb1* in APAP-induced mouse model liver tissue (Fig. 1G). Similarly, the increase in *BTF3L4* mRNA was validated in several sequencing libraries from the (Gene Expression Omnibus) GEO database, including GSE120652, GSE54257, and GSE80751 (Fig. 1H). BTF3L4 was therefore consistently overexpressed in human APAP-induced DILI and in the APAP-induced animal model. It has been reported that proliferating cell nuclear antigen (PCNA) was critically involved in regulating liver regeneration after liver injury.²⁴ Thus, PCNA is considered a classical biomarker of the degree of liver injury. Increases in *BTF3L4*, *PCNA*, and *HMGB1* mRNA were observed in AILI from GSE80751 (Fig. 1I, J). In addition, we confirmed that *BTF3L4* was highly correlated with *HMGB-1* (Fig. 1K). The correlation coefficients were 0.74. The area under the receiver operating characteristic curve was used to measure prognostic accuracy,²⁵ and for *BTF3L4* it was 0.788, suggesting that *BTF3L4* may be a potential biomarker for the detection of AILI (Fig. 1L). Therefore, the findings indicate that BTF3L4 may increase the risk of AILI by regulating inflammation.

BTF3L4 is positively correlated with hepatic injury in APAP-induced mouse model

To further assess the pathogenic effect of BTF3L4, we used a mouse model in which liver injury was induced by administering a nonlethal 300 mg/kg dose of APAP, and we monitored mortality for 3 days. Survival decreased after administration of APAP, and was 80% at 48 h. Liver sam-

ples were collected from the mice at 6, 24, and 48 h after APAP treatment for evaluation of HE-stained tissues (Fig. 2A). Expression of liver injury-related proteins and inflammatory cytokines was significantly increased 6 h after APAP treatment compared with controls (Fig. 2B). Moreover, in liver tissue from the APAP-induced model mice the trend of BTF3L4 expression was consistent with the trends of liver injury-related protein and inflammatory cytokine expressions (Fig. 2B). The immunohistochemical analysis of TUNEL staining (Fig. 2C, E) and area of liver necrosis (Fig. 2A, D) also indicated much more severe responses in mice at both 6 and 24 h after APAP administration than seen in controls. Consistent with the above indicators of liver injury, the expression of BTF3L4 was positively correlated with the number of TUNEL⁺ cells in APAP-induced mouse model (Fig. 2F). In summary, BTF3L4 may enhance APAP-evoked liver damage in APAP-induced mouse model.

BTF3L4 regulates hepatic injury in AML-12 cells

To investigate the explicit function of BTF3L4 in normal hepatocytes, we constructed an AML-12 cell line stably expressing BTF3L4 (Fig. 3A). BTF3L4 expression promoted the degree of hepatocellular necrosis, apoptosis and inflammation, as shown by the quantitative analysis of related proteins and inflammatory cytokines (Fig. 3A, D–G). Conversely, knockdown of BTF3L4 in AML-12 cells by shRNA inhibited the degree of hepatocellular injury-related protein expression compared with shControl (Fig. 3A). Moreover, correlation analysis of BTF3L4 and liver injury-related protein or TNF- α protein expression showed that the protein expression of BTF3L4 was positively correlated with liver injury-related protein in the AML-12 cell line (Fig. 3B, C). Overall, the results suggest that BTF3L4 regulated hepatic injury by necrosis, apoptosis, and inflammation in normal mouse hepatocytes.

Overexpression of BTF3L4 accelerates cellular injury in the APAP-induced cellular model

To address the potential impact of time on the ability of APAP to influence cell viability, AML-12 cells were cultured with media containing 30 mM APAP for 7 h. Subsequently, CCK8 assay showed that the cell viability dropped to 50% compared with control at the time of culturing with APAP after 3 h (Fig. 4A). In agreement with previous research, the expression of liver injury-related and inflammation-related proteins significantly increased after treating with APAP (Fig. 4B, C). We also found that the protein expression of BTF3L4 was positively correlated with liver injury-related proteins and inflammatory cytokines after 3 h of APAP treatment (Fig. 4D). To further define the role of BTF3L4 in APAP-induced cellular model, the AML-12 cell lines of BTF3L4 overexpression or knockdown were cultured with media containing 30 mM APAP for 3 h. We observed that the expression of liver injury-related and inflammation-related proteins significantly increased in BTF3L4 overexpressing cells with 3 h of APAP treatment, but in BTF3L4 knockdown cells not all changes were significant at 3 h compared with controls (Fig. 4E, F). In BTF3L4 gene-operated cells treated with APAP, the trend of BTF3L4 protein expression at 3 h was consistent with p-JNK expression. According to previous studies, p-JNK promotes increased mitochondrial ROS production and forms a self-sustaining activation loop to damage hepatic cells during AILI.⁶ In addition, BTF3L4 mediated the mRNA expression levels of IL-1 β and TNF- α inflammatory cytokines in the APAP-induced cellular model after 3 h of APAP treatment (Fig. 4G). The level of BTF3L4 mRNA was positively correlated with levels of inflammatory cytokines in the APAP-induced cellular model after 3 h of APAP treatment (Fig. 4H). Collectively, the data demon-

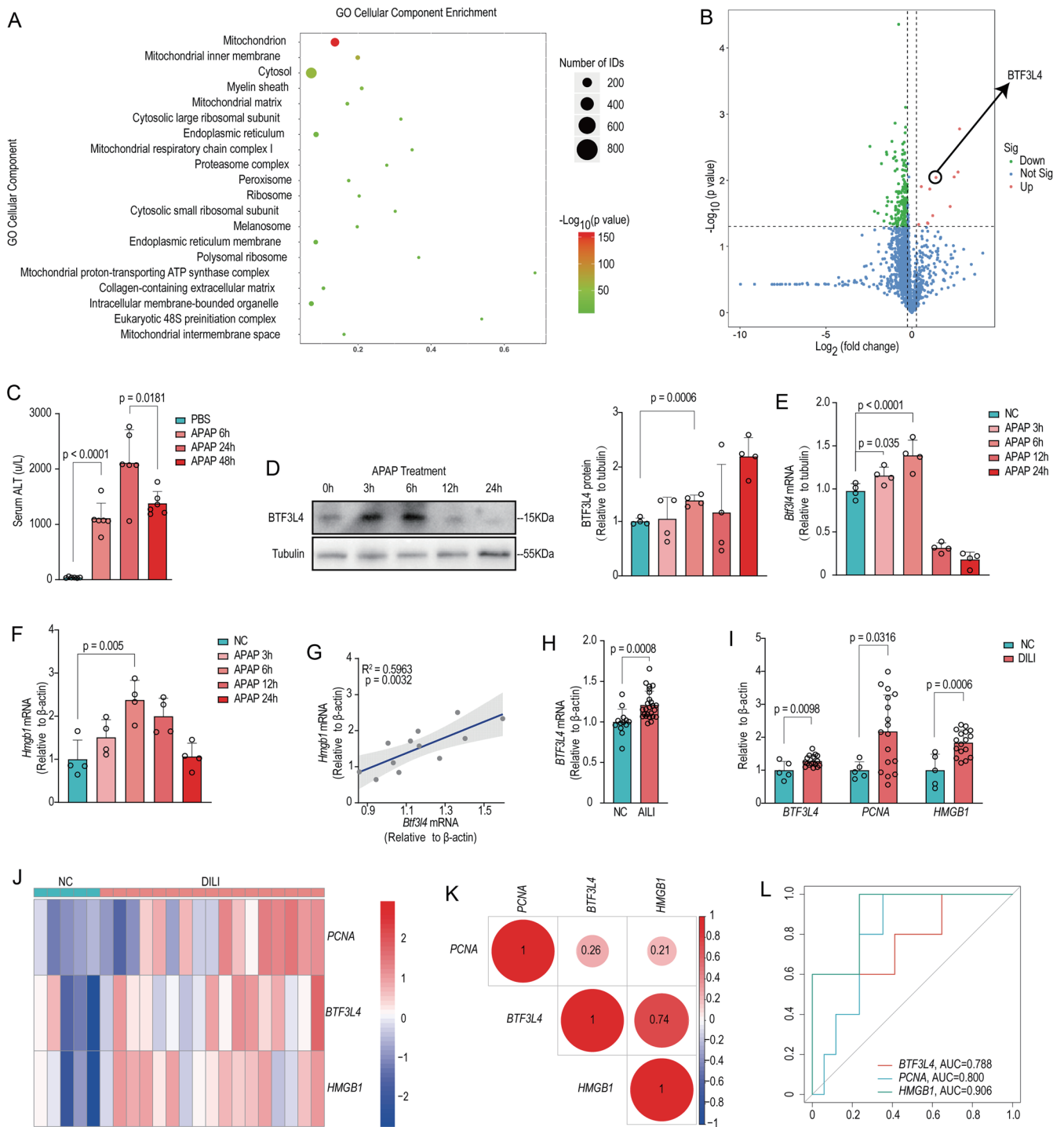


Fig. 1. BTF3L4 is overexpressed in acetaminophen-induced liver injury. (A) Proteomic analysis of four paired APAP-induced mouse models and normal mouse liver tissues. BTF3L4 was the only transcription factor among the upregulated proteins. (B) GO cellular component enrichment mitochondrial was the top changed cellular component among APAP-induced mouse liver tissues. (C) Serum ALT of mice under APAP treatment at 6, 24, and 48 h ($n=4$). (D) BTF3L4 protein expression in APAP-induced mouse model and normal mouse liver tissue ($n=4$). (E) *Btf3l4* mRNA expression in APAP-induced mouse model and normal mouse liver tissue ($n=4$). (F) *Hmgb1* mRNA expression in APA- induced mouse model and normal mouse liver tissue ($n=4$). (G) Analysis of correlation between *Btf3l4* and *Hmgb1* mRNA expression in APAP-induced mouse liver tissue. (H) *Btf3l4* mRNA expression in several sequencing libraries from the GEO database. (I) *BTF3L4*, *PCNA*, and *HMGB1* mRNA expression in GSE80751 from GEO database. (J) Heat maps show the mRNA expression levels of *BTF3L4* and *HMGB-1*, and *PCNA* in normal and drug liver samples. (K) Pearson correlation analysis of *BTF3L4*, *HMGB-1*, and *PCNA* in patients with AILI. (L) ROC curves and AUCs of *BTF3L4*, *PCNA*, and *HMGB-1* in AILI. Data are means \pm standard error of the means. Paired two-tailed Student's *t*-tests were used. BTF3L4, Basic Transcription Factor 3 Like 4; APAP, Acetaminophen; GO, Gene Ontology; ALT, Alanine aminotransferase; Hmgb1, High mobility group box-1 protein; GEO, Gene Expression Omnibus; PCNA, Proliferating cell nuclear antigen; AILI, Acetaminophen-induced liver injury; ROC, Receiver operating characteristic; AUCs, Area under the receiver operating characteristic curve.

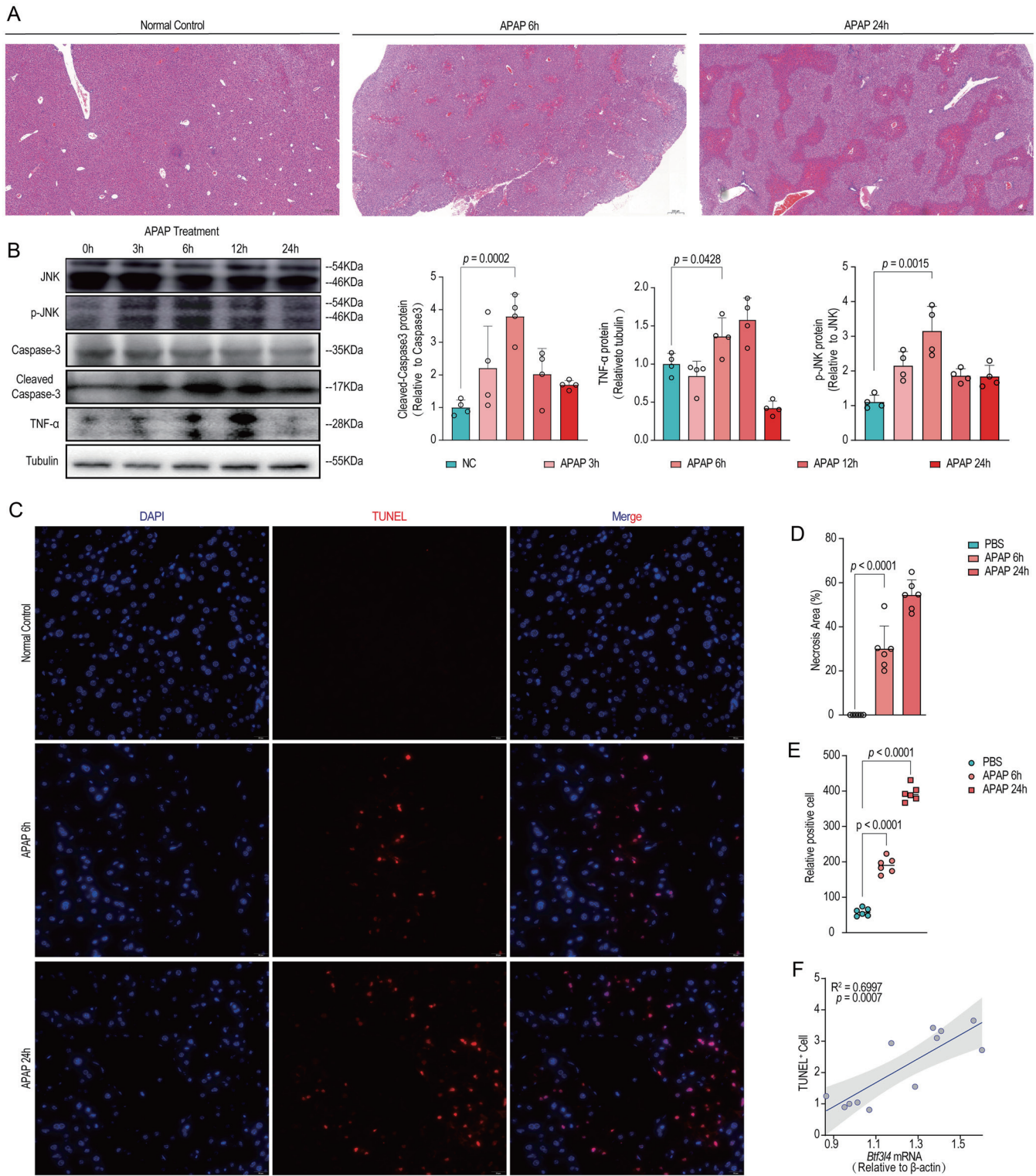


Fig. 2. BTF3L4 protein expression is positively correlated with hepatic injury in APAP-induced mouse model of liver injury. (A) Hematoxylin and eosin staining of APAP-induced mouse model and normal mouse liver tissues. (B) Caspase-3, cleaved caspase-3, p-JNK, JNK and TNF-α protein expression in APAP-induced mouse model and normal mouse liver tissues. Quantitative analysis of caspase-3, cleaved caspase-3, p-JNK, JNK, and TNF-α protein expression in APAP-induced mouse model. (C) TUNEL staining of APAP-induced mouse model and normal mouse liver tissues. (D) Necrosis area of APAP induced mouse model and normal mouse liver tissues. (E) Number of TUNEL⁺ cells in APAP-induced mouse model and normal mouse liver tissues. (F) Analysis of correlation between *BTF3L4* gene expression and TUNEL⁺ cell in APAP-induced mouse model liver tissues. Data are means±standard error of the means. (B, D, E) Paired two-tailed Student's *t*-tests were used. JNK, c-Jun N-terminal kinase; p-JNK, Phospho-c-Jun N-terminal kinase; TNF-α, Tumor Necrosis Factor-alpha; TUNEL, Terminal Deoxynucleotidyl Transferase-mediated dUTP-biotin Nick End Labeling.

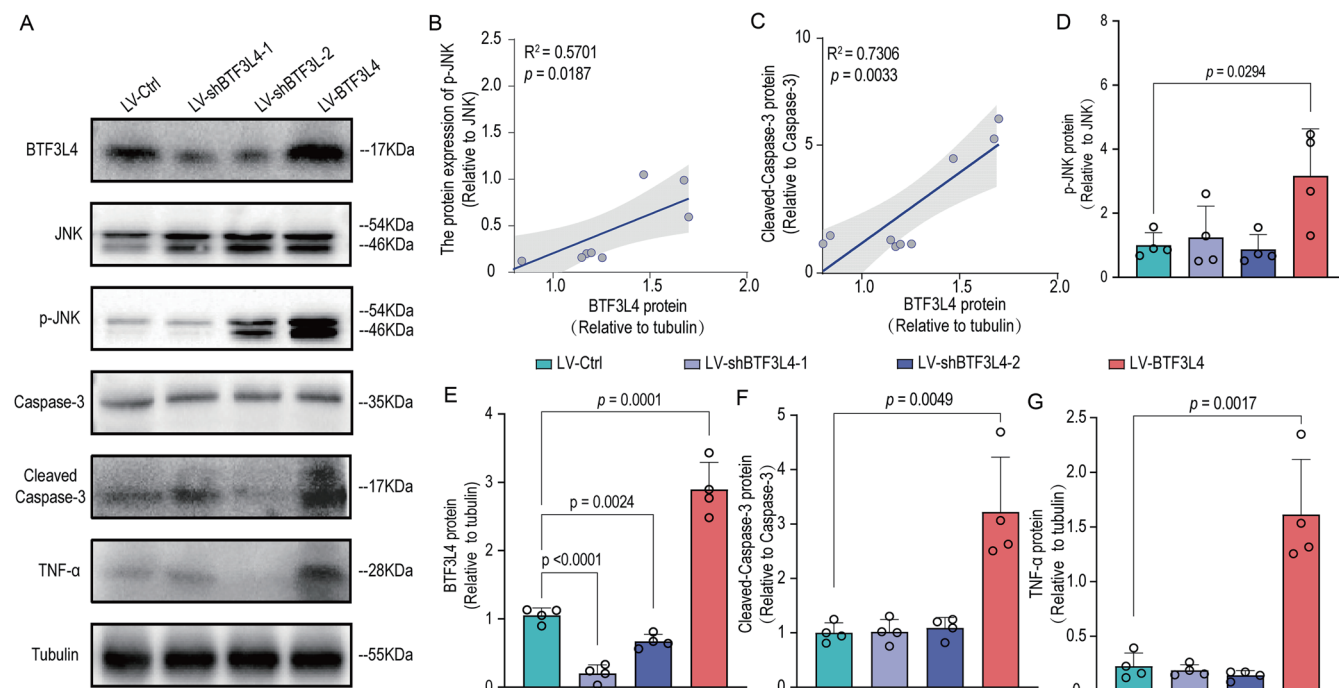


Fig. 3. BTF3L4 regulates hepatic injury in AML-12 cell line. (A) Caspase-3, cleaved caspase-3, JNK, p-JNK, and TNF- α protein expression in overexpression and knockdown of BTF3L4 in AML-12 cell lines. (B) Analysis of correlation between BTF3L4 and p-JNK protein expression in APAP-induced mouse model liver tissues. (C) Analysis of correlation between BTF3L4 and cleaved caspase-3 protein expression in APAP-induced mouse model liver tissues. (D–G) Quantitative analysis of p-JNK, BTF3L4, cleaved caspase-3, and TNF- α protein expression in AML-12 cell cells overexpressing BTF3L4 or with BTF3L4 knockdown. Data are means \pm standard error of the means. Paired two-tailed Student’s *t*-tests were used. JNK, c-Jun N-terminal kinase; p-JNK, Phospho-c-Jun N-terminal kinase; TNF- α , Tumor Necrosis Factor-alpha.

strated that increased BTF3L4 expression exacerbated AILI and promoted hepatic injury in the cellular model by inducing an inflammatory response and cell apoptosis.

A previous study reported that APAP was first metabolized in liver and generated reactive metabolites that bound to mitochondrial proteins to initiate mitochondrial damage and cause oxidative stress.¹⁷ Given the important pathogenic role of mitochondrial dysfunction in DILI, we evaluated whether BTF3L4 affected mitochondrial integrity in the APAP-induced cellular model.

Using TEM to analyze ultrastructural changes in the cellular model, we found that the mitochondria were swollen and round and that the mitochondrial cristae were disrupted by APAP administration. Mitochondria were less swollen and had well-organized cristae in BTF3L4 knockdown cells than in control cells in the APAP-induced cellular model. The opposite results were seen in cells that overexpressed BTF3L4 in the APAP-induced cellular model (Fig. 5A). Followed by the increased mitochondrial dysfunction, oxidative stress would further aggravate the accumulation of ROS, thus accelerating the inflammatory cascade. Flow cytometric analysis found a marked increase of ROS intensity in AML-12 cells overexpressing BTF3L4 (Fig. 5B). Importantly, we found that BTF3L4 regulated the levels of ROS, GSH, and TBARS in APAP-induced model cells (Fig. 5C–E). Together, the data showed that enhanced BTF3L4 expression *in vitro* disturbed mitochondrial morphology and increased the level of oxidative stress in the APAP-induced cellular model.

Previous studies indicated an important role of TNF signaling in switching damaged cells from survival toward cell death.^{26,27} Given that TNF can induce both apoptosis and cell death with features of necrosis,^{13,28,29} an increased degree of hepatic apoptosis may enhance the susceptibility to hepatic

necrosis following the activation of TNF signaling in the cellular model of APAP-induced hepatic injury. To determine the change in hepatic apoptosis by BTF3L4 in the APAP-induced cellular model, we performed TUNEL staining (Fig. 6A) and flow cytometry of AML-12 cells with BTF3L4 knockdown or overexpression in the APAP-induced cellular model (Fig. 6B). The results showed that BTF3L4 regulated hepatic injury by affecting the apoptosis level.

Discussion

The role of BTF3 in the development of digestive diseases by regulating apoptosis has been demonstrated recently.^{16–18} BTF3 regulates apoptosis and mitochondrial homeostasis in the liver, and BTF3L4, a homolog of TBF3, may have a similar function in mediating apoptosis signaling in cells.¹⁹ However, whether BTF3L4 has a role in the development of digestive diseases and its explicit mechanism remains unclear. Here, we demonstrated four major findings. (1) BTF3L4 expression was increased and positively associated with inflammation in patients with liver injury caused by APAP. (2) BTF3L4 regulated inflammation and apoptosis in mouse hepatocytes (Supplementary Fig. 1). (3) BTF3L4 overexpression aggravated liver injury by increasing the accumulation of ROS, oxidative stress, and degree of apoptosis in the AILI model. To the best of our knowledge, this is the first report to reveal that BTF3L4 expression has a role in AILI at the molecular level.

Accumulation of ROS and mitochondrial dysfunction caused by APAP leads to liver injury, forming an inflammation cascade by continuously secreting pro-inflammatory cytokines that recruit immune cells. HMGB1 is a nuclear protein released during necrosis of most cell types and acts as a damage-associated molecular pattern to activate innate immune

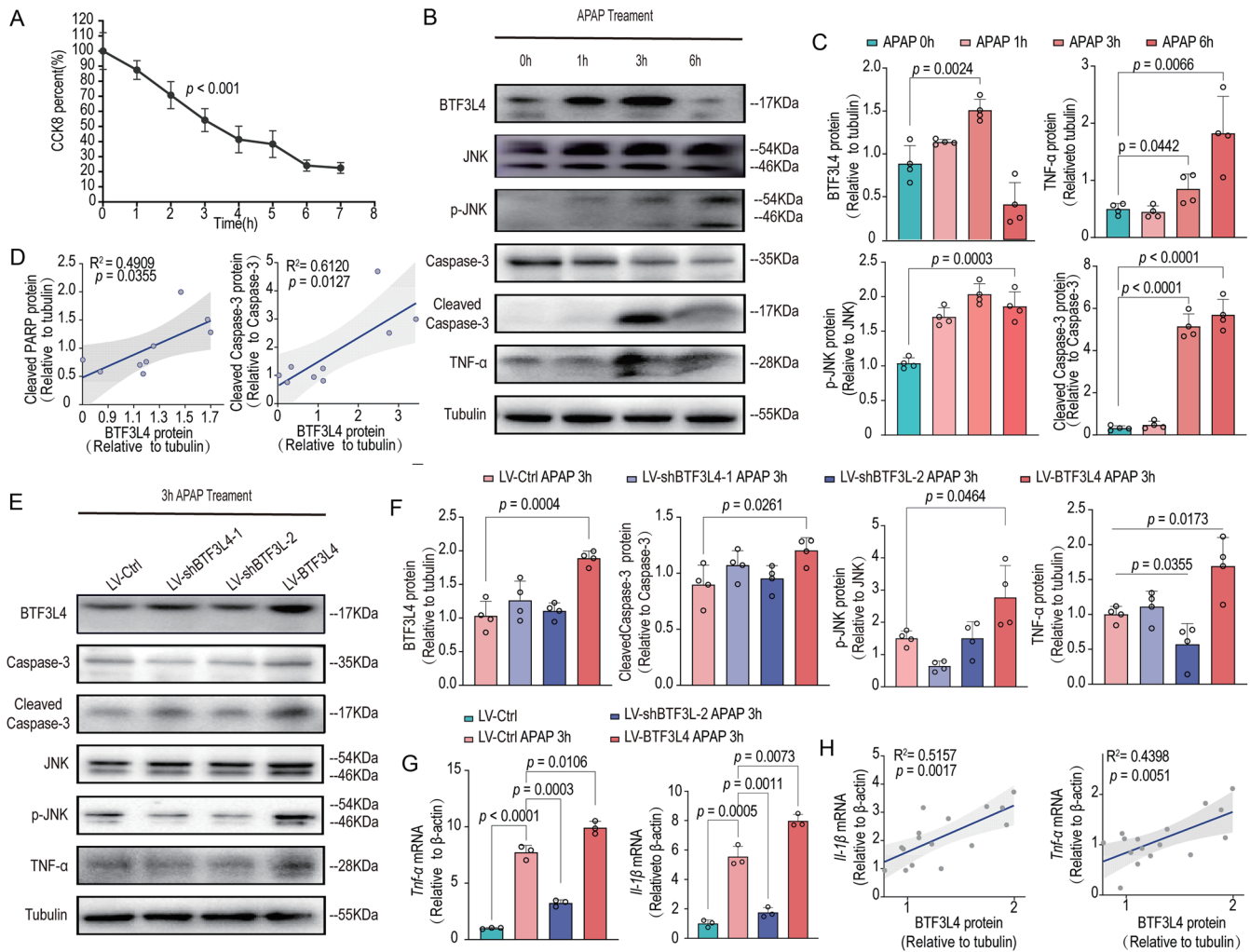


FIG. 4. Overexpression of BTF3L4 accelerates cellular injury in an APAP-induced cellular model. (A) The viability of AML-12 cells under APAP treatment is time dependent. (B) Caspase-3, cleaved caspase-3, JNK, p-JNK, and TNF- α protein expression in an APAP-induced cellular model. (C) Quantitative analysis of caspase-3, cleaved caspase-3, JNK, p-JNK, and TNF- α protein expression in an APAP-induced cellular model. (D) Analysis of correlation between BTF3L4 and liver injury-related protein expression in an APAP-induced cellular model. (E) Caspase-3, cleaved caspase-3, JNK, p-JNK, and TNF- α protein expression in AML-12 cells with BTF3L4 overexpression or knockdown after 3 h of APAP treatment. (F) Quantitative analysis of caspase-3, cleaved caspase-3, JNK, p-JNK, and TNF- α protein expression in AML-12 cells with BTF3L4 overexpression or knockdown after 3 h of APAP treatment. (G) IL-1 β and TNF- α mRNA expression in AML-12 cells with BTF3L4 overexpression or knockdown after 3 h of APAP treatment. (H) Analysis of correlation between BTF3L4 mRNA expression and inflammatory cytokines in AML-12 cells with BTF3L4 overexpression or knockdown after 3 h of APAP treatment. Data are means \pm standard error of the means. (C–H) Paired two-tailed Student’s *t*-tests were used. IL-1 β , Interleukin-1 β ; JNK, c-Jun N-terminal kinase; p-JNK, Phospho-c-Jun N-terminal kinase; TNF- α , Tumor Necrosis Factor-alpha.

cells, and is considered a possible biomarker of AILI.^{30,31} By analyzing the protein expression and proteomic analysis of the AILI model, we found that BTF3L4 expression was highly increased in the AILI model. Consistent with the AILI model, analysis of GEO data found that BTF3L4 expression was increased in patient liver tissue and had a proinflammatory role in the progression of AILI. Acting as a TF and a critical field of a nascent polypeptide-associated complex,^{32,33} BTF3L4 was predicted as an intracellular cytoplasmic-membrane protein that functions in the targeting and translocation of nascent polypeptides. It is also found in the nucleus as a TF. BTF3L4 is a homolog of TBF3 that participates in cellular inflammation by mediating apoptosis signaling in cells. However, unlike the overexpression of BTF3 in normal liver tissue, BTF3L4 was underexpressed in normal liver tissue. All the above findings indicate that BTF3L4 may participate in the pathogenesis of AILI by affecting inflammation.

In the normal liver, nearly all cells are in a state of low turnover with virtually no cell death.³⁴ Apoptosis is a programmed cell death, which has only minimal effects on the surrounding cells.³⁵ In contrast to apoptosis, necrosis has a critical role in APAP hepatotoxicity,³⁶ inducing a major inflammatory response and subsequently damaging neighboring cells. TNF can induce a change from apoptosis to necroptosis, which results in cell death with features of necrosis.¹³ Given that various cytokines and stress signals can trigger apoptotic pathways leading to irreversible apoptotic activation and ultimately cell death,³⁷ it is plausible that apoptosis may contribute to AILI. Excessively damaged mitochondria induce injury in hepatocytes from survival to cell death, including the activation of intrinsic apoptotic signaling pathways and recruitment of inflammation-related immune cells.³⁸ This process can activate the inflammatory cells in the liver, resulting in the production of large amounts

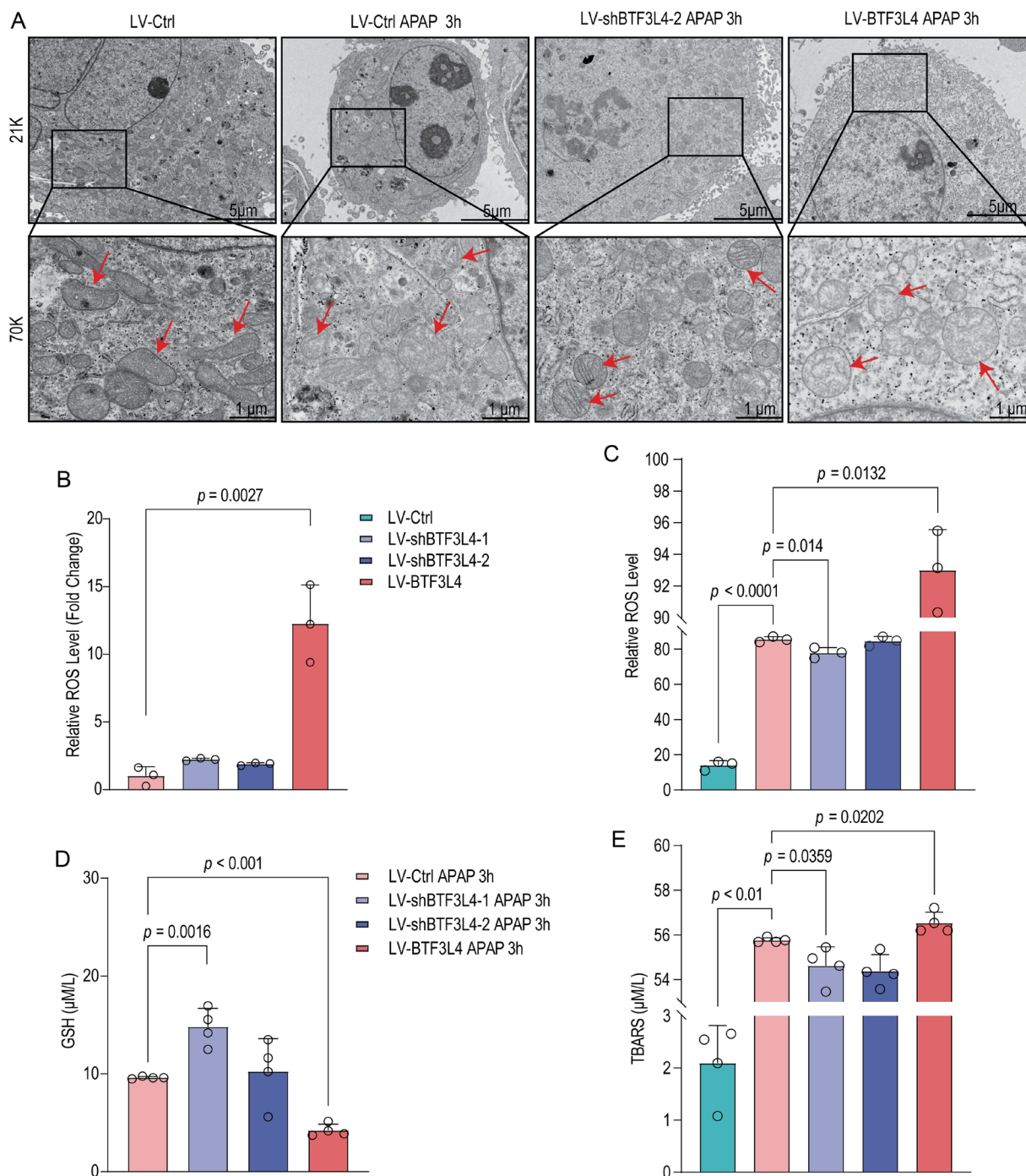


Fig. 5. BTF3L4 mediates mitochondrial morphology in an APAP-induced cellular model. (A) Representative TEMs of mitochondria in AML-12 cells with BTF3L4 overexpression or knockdown after 3 h of APAP treatment. The red arrows indicate the presence of mitochondria. (B) The level of ROS in AML-12 cells with BTF3L4 overexpression or knockdown. (C) The level of ROS in AML-12 cells with BTF3L4 overexpression or knockdown after 3 h of APAP treatment. (D) The level of GSH in AML-12 cells with BTF3L4 overexpression or knockdown after 3 h of APAP treatment. (E) The level of TBARS in AML-12 cells with BTF3L4 overexpression or knockdown after 3 h of APAP treatment. Data are means ± standard error of the means. (B–E) Paired two-tailed Student’s *t*-tests were used. TEM, Transmission Electron Microscopy; ROS, Reactive Oxygen Species; GSH, Glutathione.

of inflammatory cytokines including TNF- α . Previous reports have demonstrated a significant increase in apoptosis level and mitochondrial dysfunction in the AILI models.^{6,39} Increased apoptosis may thus reduce hepatic injury by triggering a switch to necroptosis through the activation of the

TNF signaling pathway during AILI. Consistent with previous studies,^{40,41} we found that apoptosis was increased in AILI animal and hepatic models. *In vitro*, we demonstrated that the apoptosis and TNF- α levels were regulated by BTF3L4 in normal liver cells without any treatment. Apart from the

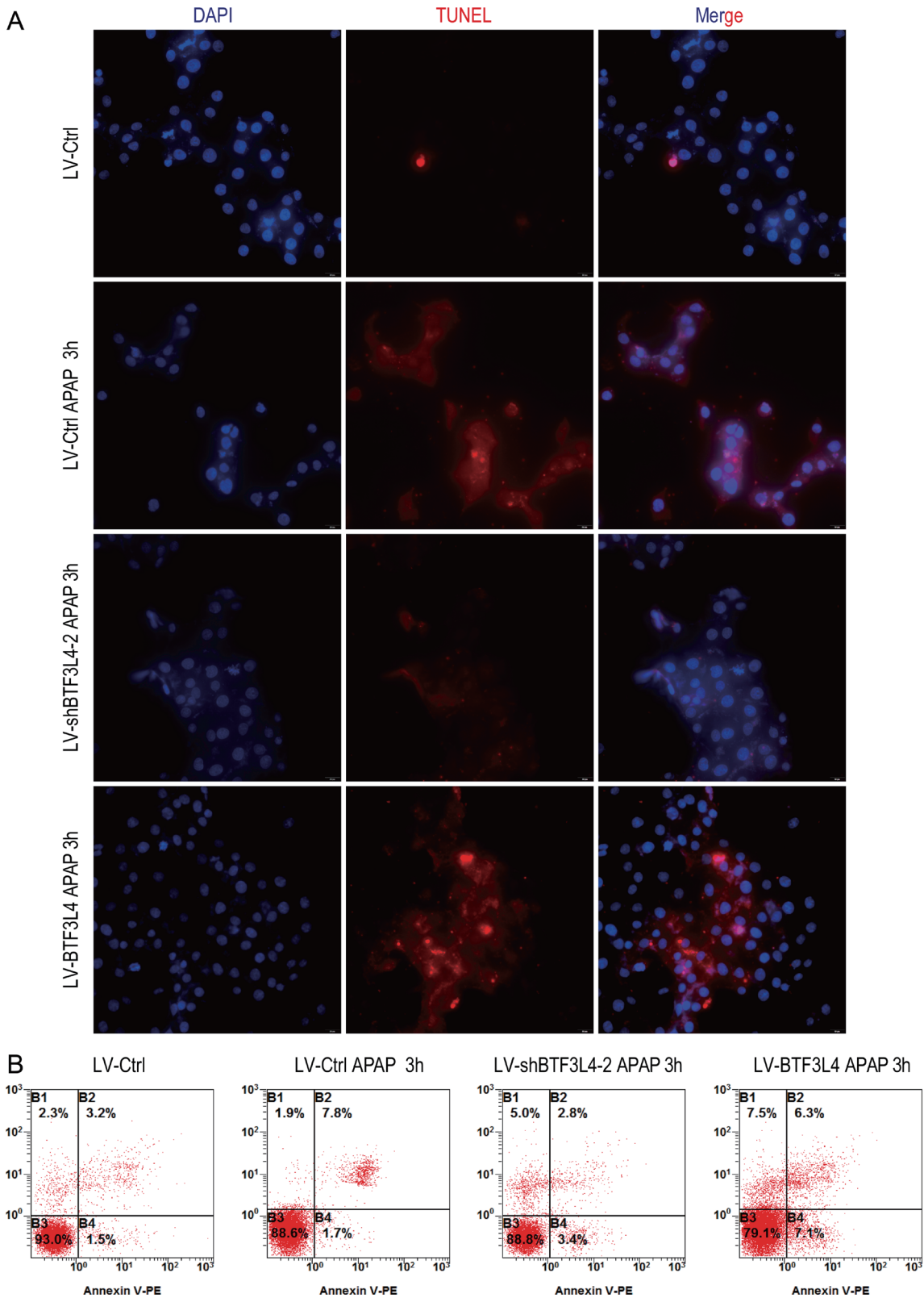


Fig. 6. BTF3L4 mediates hepatic injury in an APAP-induced cellular model. (A) TUNEL staining of BTF3L4 overexpression and knockdown cell lines after 3 h of APAP treatment. (B) Cell cycle distribution in AML-12 cells with BTF3L4 overexpression or knockdown after 3 h of APAP treatment. TUNEL, Terminal Deoxynucleotidyl Transferase-mediated dUTP-biotin Nick End Labeling;

physiological state, we also established that BTF3L4 overexpression increased apoptosis and TNF- α protein expression in the AILI cellular model. We also observed that BTF3L4 was positively associated with apoptosis and inflammation in the AILI animal model. Overall, the results show that BTF3L4 overexpression may deteriorate liver injury and accelerate the progression from apoptosis to necroptosis by regulating TNF- α levels.

N-acetyl-p-benzoquinone imine is the main metabolite of APAP, which damages mitochondrial proteins and enhances the formation of superoxide radicals in AILI progression.⁶ These superoxide radicals are directly detoxified by GSH or scavenged by several antioxidant enzymes in hepatocytes, including catalase, GSH peroxidase, and peroxiredoxin.⁴² Following an APAP overdose, GSH is exhausted by the excess of free radicals, resulting in damage to mitochondrial morphology and function. Damaged mitochondria cause liver injury by triggering an inflammatory cascade and generating excessive ROS.⁴³ Consistent with a previous study,²² our findings demonstrate a significant increase in ROS levels in the AILI cellular model. Our investigation also revealed deterioration in mitochondrial morphology in hepatic cells subjected to APAP treatment, reflecting mitochondrial dysfunction to some degree. Subsequently, we found that BTF3L4 mediated ROS, GSH, and TBARS, the level of inflammatory cytokine mRNAs, and mitochondrial morphology *in vitro*. In AILI progression, oxidative stress caused by mitochondrial dysfunction may initiate several molecules and signaling pathways to aggravate liver injury. An excess of ROS triggers apoptosis-related signaling to activate JNK.⁴⁴ Sustained activation of JNK increases mitochondrial ROS production and forms a self-sustaining activation loop. Because of the deterioration of mitochondrial integrity, a series of apoptosis-inducing factors are translocated to the nucleus, resulting in DNA fragmentation and subsequently necrosis.⁴⁵ Given the function of BTF3L4 in regulating ROS accumulation and inflammation in the AILI model, BTF3L4 may play a pathogenic role in AILI by affecting mitochondrial function and mitochondria-mediated inflammation.

In conclusion, our results indicate that BTF3L4 regulated apoptosis and inflammation in normal hepatocytes and that enhancement of BTF3L4 promotes the accumulation of ROS, oxidative stress and apoptosis degree in the AILI model. The study provides evidence that BTF3L4 aggravates liver injury during the progression of AILI by deteriorating mitochondrial function and mitochondria-mediated inflammation. Further studies in different DILI models are required to better understand the mechanism of BTF3L4 in AILI using RNA sequencing. Our results suggest that BTF3L4 overexpression is involved in the pathogenesis of liver injury by mediating mitochondrial function and inflammation. BTF3L4 is a pathogenic factor in AILI, and the use of BTF3L4 inhibitors may be a promising approach for the prevention and treatment of AILI.

Acknowledgments

We sincerely thank the GEO databases for their generous support of this study by providing us with a large amount of data. We thank Liu Hong for providing meaningful advice regarding the implementation of this study.

Funding

This research was funded by Independent Funds of the Key Laboratory (CBSKL2022ZZ34) and Xijing Hospital Booster Program (XJZT21CM04).

Conflict of interest

The authors have no conflicts of interest related to this publication.

Author contributions

Conceptualization and methodology (JL, ZY), data validation and formal analysis (JL, AF, QX), original draft preparation (JL, WZ, AF), and overall editing and supervision (LH, WZ). All authors have read and agreed to the published version of the manuscript.

Ethical statement

This study was carried out in accordance with the recommendations in the Guide for the Care and Use of Laboratory Animals of the National Institutes of Health. The protocol was approved by the Institutional of the Animal Center of the Fourth Military Medical University (No. SCXK2012-0007).

Data sharing statement

The data used and analyzed in this study are available from the corresponding authors, upon reasonable request.

References

- Fontana RJ, Bjornsson ES, Reddy R, Andrade RJ. The Evolving Profile of Idiosyncratic Drug-Induced Liver Injury. *Clin Gastroenterol Hepatol* 2023;21(8):2088–2099. doi:10.1016/j.cgh.2022.12.040, PMID:36868489.
- Boeckmans J, Rodrigues RM, Demuyser T, Piérard D, Vanhaecke T, Rogiers V. COVID-19 and drug-induced liver injury: a problem of plenty or a petty point? *Arch Toxicol* 2020;94(4):1367–1369. doi:10.1007/s00204-020-02734-1, PMID:32266419.
- Saleh NEH, Saad AH, Elbassuoni EA, El-Tahawy NF, Abdel-Hakeem EA. Potential benefits of using hydrogen sulfide, vitamin E and necrostatin-1 to counteract acetaminophen-induced hepatotoxicity in rats. *Bratisl Lek Listy* 2021;122(10):732–738. doi:10.4149/BLL_2021_117, PMID:34570575.
- Kobayashi T, Iwaki M, Nogami A, Yoneda M. Epidemiology and Management of Drug-Induced Liver Injury: Importance of the Updated RUCAM. *J Clin Transl Hepatol* 2023;11(5):1239–1245. doi:10.14218/JCTH.2022.000675, PMID:37577239.
- Li X, Tang J, Mao Y. Incidence and risk factors of drug-induced liver injury. *Liver Int* 2022;42(9):1999–2014. doi:10.1111/liv.15262, PMID:35353431.
- Yan M, Huo Y, Yin S, Hu H. Mechanisms of acetaminophen-induced liver injury and its implications for therapeutic interventions. *Redox Biol* 2018;17:274–283. doi:10.1016/j.redox.2018.04.019, PMID:29753208.
- Hoofnagle JH, Björnsson ES. Drug-Induced Liver Injury - Types and Phenotypes. *N Engl J Med* 2019;381(3):264–273. doi:10.1056/NEJMra1816149, PMID:31314970.
- Chilvery S, Yelne A, Khurana A, Saifi MA, Bansod S, Anchi P, *et al*. Acetaminophen induced hepatotoxicity: An overview of the promising protective effects of natural products and herbal formulations. *Phytomedicine* 2023;108:154510. doi:10.1016/j.phymed.2022.154510, PMID:36332383.
- Lee J, Ha J, Kim JH, Seo D, Kim M, Lee Y, *et al*. Peli3 ablation ameliorates acetaminophen-induced liver injury through inhibition of GSK3 β phosphorylation and mitochondrial translocation. *Exp Mol Med* 2023;55(6):1218–1231. doi:10.1038/s12276-023-01009-w, PMID:37258579.
- Raucy JL, Lasker JM, Lieber CS, Black M. Acetaminophen activation by human liver cytochromes P450IIE1 and P450IA2. *Arch Biochem Biophys* 1989;271(2):270–283. doi:10.1016/0003-9861(89)90278-6, PMID:272995.
- Jaeschke H. Emerging novel therapies against paracetamol (acetaminophen) hepatotoxicity. *EBioMedicine* 2019;46:9–10. doi:10.1016/j.ebiom.2019.07.054, PMID:31350222.
- Win S, Than TA, Min RW, Aghajani M, Kaplowitz N. c-Jun N-terminal kinase mediates mouse liver injury through a novel Sab (SH3BP5)-dependent pathway leading to inactivation of intramitochondrial Src. *Hepatology* 2016;63(6):1987–2003. doi:10.1002/hep.28486, PMID:26845758.
- Schwabe RF, Luedde T. Apoptosis and necroptosis in the liver: a matter of life and death. *Nat Rev Gastroenterol Hepatol* 2018;15(12):738–752. doi:10.1038/s41575-018-0065-y, PMID:30250076.
- Gorman GS, Chinnery PF, DiMauro S, Hirano M, Koga Y, McFarland R, *et al*. Mitochondrial diseases. *Nat Rev Dis Primers* 2016;2:16080. doi:10.1038/nrdp.2016.80, PMID:27775730.
- Jamil M, Wang W, Xu M, Tu J. Exploring the roles of basal transcription factor 3 in eukaryotic growth and development. *Biotechnol Genet Eng Rev* 2015;31(1-2):21–45. doi:10.1080/02648725.2015.1080064, PMID:26428578.
- Huang P, Xia L, Guo Q, Huang C, Wang Z, Huang Y, *et al*. Genome-wide

- association studies identify miRNA-194 as a prognostic biomarker for gastrointestinal cancer by targeting ATP6V1F, PPP1R14B, BTF3L4 and SLC7A5. *Front Oncol* 2022;12:1025594. doi:10.3389/fonc.2022.1025594, PMID:36620589.
- [17] Zhang Y, Gao X, Yi J, Sang X, Dai Z, Tao Z, *et al*. BTF3 confers oncogenic activity in prostate cancer through transcriptional upregulation of Replication Factor C. *Cell Death Dis* 2021;12(1):12. doi:10.1038/s41419-020-03348-2, PMID:33414468.
- [18] Zhang DZ, Chen BH, Zhang LF, Cheng MK, Fang XJ, Wu XJ. Basic Transcription Factor 3 Is Required for Proliferation and Epithelial-Mesenchymal Transition via Regulation of FOXM1 and JAK2/STAT3 Signaling in Gastric Cancer. *Oncol Res* 2017;25(9):1453–1462. doi:10.3727/096504017X14886494526344, PMID:28276310.
- [19] Zhang L, Dong L, Yang L, Luo Y, Chen F. MiR-27a-5p regulates acrylamide-induced mitochondrial dysfunction and intrinsic apoptosis via targeting Btf3 in rats. *Food Chem* 2022;368:130816. doi:10.1016/j.foodchem.2021.130816, PMID:34416489.
- [20] Zeng KW, Wang JK, Wang LC, Guo Q, Liu TT, Wang FJ, *et al*. Small molecule induces mitochondrial fusion for neuroprotection via targeting CK2 without affecting its conventional kinase activity. *Signal Transduct Target Ther* 2021;6(1):71. doi:10.1038/s41392-020-00447-6, PMID:33602894.
- [21] Gong S, Lan T, Zeng L, Luo H, Yang X, Li N, *et al*. Gut microbiota mediates diurnal variation of acetaminophen induced acute liver injury in mice. *J Hepatol* 2018;69(1):51–59. doi:10.1016/j.jhep.2018.02.024, PMID:29524531.
- [22] Zheng J, Zhou H, Yang T, Liu J, Qin T, Gu X, *et al*. Protective Role of microRNA-31 in Acetaminophen-Induced Liver Injury: A Negative Regulator of c-Jun N-Terminal Kinase (JNK) Signaling Pathway. *Cell Mol Gastroenterol Hepatol* 2021;12(5):1789–1807. doi:10.1016/j.jcmgh.2021.07.011, PMID:34311140.
- [23] Zhang Z, Xu X, Tian W, Jiang R, Lu Y, Sun Q, *et al*. ARRB1 inhibits non-alcoholic steatohepatitis progression by promoting GDF15 maturation. *J Hepatol* 2020;72(5):976–989. doi:10.1016/j.jhep.2019.12.004, PMID:31857195.
- [24] Sherr CJ. G1 phase progression: cycling on cue. *Cell* 1994;79(4):551–555. doi:10.1016/0092-8674(94)90540-1, PMID:7954821.
- [25] Narayan HK, French B, Khan AM, Plappert T, Hyman D, Bajulaiye A, *et al*. Noninvasive Measures of Ventricular-Arterial Coupling and Circumferential Strain Predict Cancer Therapeutics-Related Cardiac Dysfunction. *JACC Cardiovasc Imaging* 2016;9(10):1131–1141. doi:10.1016/j.jcmg.2015.11.024, PMID:27085442.
- [26] Wree A, Eguchi A, McGeough MD, Pena CA, Johnson CD, Canbay A, *et al*. NLRP3 inflammasome activation results in hepatocyte pyroptosis, liver inflammation, and fibrosis in mice. *Hepatology* 2014;59(3):898–910. doi:10.1002/hep.26592, PMID:23813842.
- [27] Bialik S, Kimchi A. Lethal weapons: DAP-kinase, autophagy and cell death: DAP-kinase regulates autophagy. *Curr Opin Cell Biol* 2010;22(2):199–205. doi:10.1016/j.cob.2009.11.004, PMID:20005690.
- [28] Alegre F, Pelegrin P, Feldstein AE. Inflammasomes in Liver Fibrosis. *Semin Liver Dis* 2017;37(2):119–127. doi:10.1055/s-0037-1601350, PMID:28564720.
- [29] Angeli JPF, Shah R, Pratt DA, Conrad M. Ferroptosis Inhibition: Mechanisms and Opportunities. *Trends Pharmacol Sci* 2017;38(5):489–498. doi:10.1016/j.tips.2017.02.005, PMID:28363764.
- [30] Yang T, Wang H, Wang X, Li J, Jiang L. The Dual Role of Innate Immune Response in Acetaminophen-Induced Liver Injury. *Biology (Basel)* 2022;11(7):1057. doi:10.3390/biology11071057, PMID:36101435.
- [31] Andrade RJ, Chalasani N, Björnsson ES, Suzuki A, Kullak-Ublick GA, Watkins PB, *et al*. Drug-induced liver injury. *Nat Rev Dis Primers* 2019;5(1):58. doi:10.1038/s41572-019-0105-0, PMID:31439850.
- [32] Addison WN, Pellicelli M, St-Arnaud R. Dephosphorylation of the transcriptional cofactor NACA by the PP1A phosphatase enhances cJUN transcriptional activity and osteoblast differentiation. *J Biol Chem* 2019;294(20):8184–8196. doi:10.1074/jbc.RA118.006920, PMID:30948508.
- [33] Jomaa A, Gamberdinger M, Hsieh HH, Wallisch A, Chandrasekaran V, Ulusoy Z, *et al*. Mechanism of signal sequence handover from NAC to SRP on ribosomes during ER-protein targeting. *Science* 2022;375(6583):839–844. doi:10.1126/science.abi6459, PMID:35201867.
- [34] Benedetti A, Jézéquel AM, Orlandi F. Preferential distribution of apoptotic bodies in acinar zone 3 of normal human and rat liver. *J Hepatol* 1988;7(3):319–324. doi:10.1016/s0168-8278(88)80004-7, PMID:3235800.
- [35] McIlwain DR, Berger T, Mak TW. Caspase functions in cell death and disease. *Cold Spring Harb Perspect Biol* 2013;5(4):a008656. doi:10.1101/cshperspect.a026716, PMID:25833847.
- [36] McGill MR, Sharpe MR, Williams CD, Taha M, Curry SC, Jaeschke H. The mechanism underlying acetaminophen-induced hepatotoxicity in humans and mice involves mitochondrial damage and nuclear DNA fragmentation. *J Clin Invest* 2012;122(4):1574–1583. doi:10.1172/JCI59755, PMID:22378043.
- [37] Yue J, López JM. Understanding MAPK Signaling Pathways in Apoptosis. *Int J Mol Sci* 2020;21(7):2346. doi:10.3390/ijms21072346, PMID:32231094.
- [38] Torres S, Baulies A, Insausti-Urkia N, Alarcón-Vila C, Fucho R, Solsona-Vilarasa E, *et al*. Endoplasmic Reticulum Stress-Induced Upregulation of STARD1 Promotes Acetaminophen-Induced Acute Liver Failure. *Gastroenterology* 2019;157(2):552–568. doi:10.1053/j.gastro.2019.04.023, PMID:31029706.
- [39] Jaeschke H, Duan L, Akakpo JY, Farhood A, Ramachandran A. The role of apoptosis in acetaminophen hepatotoxicity. *Food Chem Toxicol* 2018;118:709–718. doi:10.1016/j.fct.2018.06.025, PMID:29920288.
- [40] Wang Y, Tian L, Wang Y, Zhao T, Khan A, Wang Y, *et al*. Protective effect of Que Zui tea hot-water and aqueous ethanol extract against acetaminophen-induced liver injury in mice via inhibition of oxidative stress, inflammation, and apoptosis. *Food Funct* 2021;12(6):2468–2480. doi:10.1039/d0fo02894k, PMID:33650604.
- [41] Hu B, Li J, Gong D, Dai Y, Wang P, Wan L, *et al*. Long-Term Consumption of Food-Derived Chlorogenic Acid Protects Mice against Acetaminophen-Induced Hepatotoxicity via Promoting PINK1-Dependent Mitophagy and Inhibiting Apoptosis. *Toxics* 2022;10(11):665. doi:10.3390/toxics10110665, PMID:36355956.
- [42] Cover C, Mansouri A, Knight TR, Bajt ML, Lemasters JJ, Pessayre D, *et al*. Peroxynitrite-induced mitochondrial and endonuclease-mediated nuclear DNA damage in acetaminophen hepatotoxicity. *J Pharmacol Exp Ther* 2005;315(2):879–887. doi:10.1124/jpet.105.088898, PMID:16081675.
- [43] Jaeschke H, McGill MR, Ramachandran A. Oxidant stress, mitochondria, and cell death mechanisms in drug-induced liver injury: lessons learned from acetaminophen hepatotoxicity. *Drug Metab Rev* 2012;44(1):88–106. doi:10.3109/03602532.2011.602688, PMID:22229890.
- [44] Gunawan BK, Liu ZX, Han D, Hanawa N, Gaarde WA, Kaplowitz N. c-Jun N-terminal kinase plays a major role in murine acetaminophen hepatotoxicity. *Gastroenterology* 2006;131(1):165–178. doi:10.1053/j.gastro.2006.03.045, PMID:16831600.
- [45] Woolbright BL, Jaeschke H. Role of the inflammasome in acetaminophen-induced liver injury and acute liver failure. *J Hepatol* 2017;66(4):836–848. doi:10.1016/j.jhep.2016.11.017, PMID:27913221.